Supporting Information

An Estrogen Receptor Targeted Ruthenium Complex as a Two-Photon Photodynamic Therapy Agent for Breast Cancer Cells

Xueze Zhao, Mingle Li, Wen Sun, Jiangli Fan*, Jianjun Du and Xiaojun Peng

State Key Laboratory of Fine Chemicals, Dalian University of Technology, Dalian 116024 China.

Correspondence and requests for materials should be addressed to J. F. (e-mail: fanjl@dlut.edu.cn)

Materials and Methods

The general chemicals used in the report were purchased from Energy Chemical Co., Aldrich Chemical Co. and J&K Scientific Ltd., and all of the solvents were of analytic grade. MTT (3-(4,5-dimethyl-2-thiazolyl)-2,5-diphenyl-2-H-tetrazolium bromide) and AO (acridine orange) were purchased from Energy Chemical Co. LysoTracker Green DND 26, Hoechst 33342 and MitoTracker Green FM were purchased from Life Technologies Co. (USA). DCFH-DA (2, 7-dichlorofluorescein diacetate) Detection Kit and calcein AM/propidium iodide (PI) Detection Kit were purchased from Beyotime Biotechnology Co. (China). JC-1 Detection Kit and Annexin V-FITC/propidium iodide (PI) Apoptosis Detection Kit were purchased from KeyGEN BioTECH Ltd. Human breast cancer MCF-7 cells, African green monkey kidney

COS-7 cells, Human breast cancer MDA-MB-231 cell and Human hepatocyte HL-7702 cells were purchased from Institute of Basic Medical Sciences (IBMS) of the Chinese Academy of Medical Sciences. All cell experiments were performed in accordance with guidelines approved by the ethics committee of Dalian Medical University.

Before the experiments, **Ru-tmxf**, **Ru-OMe** and tamoxifen were dissolved in dimethyl sulfoxide (DMSO), and the final concentration of DMSO was less than 1% (v/v).NMR spectra of **Ru-tmxf** and **Ru-OMe** were detected by Bruker Avance III 500 spectrometer. Mass spectrometric (ESI-MS) data were obtained with LTQ Orbitrap XL and TSQ Quantum Ultra system. Fluorescence measurements were performed on a VAEIAN CARY Eclipse fluorescence spectrophotometer (Serial No. FL0812-M018). Fluorescence quantum yield was obtained with the HAMAMATSU absolute fluorescence quantum yield spectrometer (Serial No. C11347).

Synthesis of Ru-OMe and Ru-tmxf

According to the literature methods.[1-3] cis-$Ru(phen)_2Cl_2 \cdot 2H_2O$ and tamoxifen ligand **2** were prepared.

Synthesis of the ligands ($\mathbf{L_1}$)

Dissolving the mixture of 1,10-phenanthroline-5,6-dione (0.42 g, 2 mmol), ammonium acetate (1.852 g, 24 mmol), aniline (0.224 g, 2.4 mmol) and anisic

aldehyde (0.272 g, 2 mmol) in glacial acetic acid (15 mL) and refluxing overnight under an argon atmosphere. After the reaction, pouring the mixture into water (20 mL), treating with a 25% ammonia until the pH = 6, giving rise to a thick dark yellow suspension. Then, Stirred the suspension and filtered to yield a dark grey crude product, the solid was purified by silica gel chromatography with CH_2Cl_2/CH_3OH (80:1, v/v), affording a yellow powder (Yield = 65%). ^{1}H NMR (500 MHz, CD_3OD) δ 9.07−9.11 (m, 2H), 8.92-8.94 (dd, *J* = 1.5, 4.0 Hz, 1H), 7.85−7.87 (m, 1H), 7.64−7.75 (m, 5H), 7.53-7.54 (d, *J* = 5.0 Hz, 2H), 7.48-7.50 (dd, *J* = 1.5, 8.5 Hz, 1H), 7.38-7.41 (m, 1H), 6.91-6.93 (d, *J* =10.0 Hz, 2H), 3.82 (s, 3H). ESI-MS: $[M + H]^+$ 403.15, found 403.19; $[2M + Na]^+$ 827.29, found 827.27.

Synthesis of the ligands (**L_2**)

Dissolving the mixture of 1,10-phenanthroline-5,6-dione (0.21 g, 1 mmol), ammonium acetate (0.926 g, 12 mmol), aniline (0.112 g, 1.2 mmol) and 4-(2-azidoethoxy) benzaldehyde (0.20 g, 1.1 mmol) in glacial acetic acid (8 mL) and refluxing overnight under an argon atmosphere. After the reaction, pouring the mixture into water (10 mL) and treating with a 25% ammonia until the pH = 6, giving rise to a thick dark green suspension. Then added $CHCl_3$ (10 mL) to the suspension, stirred and filtered to yield a gray crude product. The solid was purified by silica gel chromatography with CH_2Cl_2/CH_3OH (40:1, v/v), affording a white powder (Yield = 70%). ^{1}H NMR (500 MHz, $CDCl_3$) δ 9.19−9.20 (dd, *J* = 2.0, 5.5 Hz 1H), 9.13-9.16 (dd, *J* = 2, 10 Hz, 1H), 9.04−9.05 (dd, *J* = 2, 5 Hz, 1H), 7.74−7.77 (m, 1H), 7.63-7.69

(m, 3H), 7.52-7.54 (d, *J* = 10.5 Hz, 4H), 7.42-7.45 (dd, *J* = 2.0, 10.5 Hz 1H), 7.26-7.31 (m, 1H), 6.84-6.86 (d, *J* = 11 Hz, 2H), 4.13-4.15 (t, *J* = 6 Hz, 2H), 3.58-3.61 (t, *J* = 6 Hz, 2H). ESI-MS: $[M + H]^+$ 458.17, found 458.03.

Synthesis of **Ru-OMe**

$Ru(phen)_2Cl_2 \cdot 2H_2O$ (0.053 g, 0.1 mmol) and $\mathbf{L_1}$ (0.040 g, 0.1 mmol) were dissolved in 10 mL ethanol and 5 mL H_2O refluxed 24 h under an argon atmosphere to give a clear red solution. After the solvent was removed, an orange-red powder was obtained. The crude product was purified by column chromatography on a neutral alumina with CH_2Cl_2/CH_3OH (25:1, v/v). The final product (orange-red soild) was obtained by adding saturated aqueous NH_4PF_6 solution dropwise to the solution of the pure product. (Yield = 78 %). ^{1}H NMR (500 MHz, $(CD_3)_2SO$) δ 9.19−9.20 (dd, *J* = 2.0, 5.5 Hz, 1H), 9.13-9.16 (dd, *J* = 2, 10 Hz, 1H), 9.04−9.05 (dd, *J* = 2, 5 Hz, 1H), 7.74−7.77 (m, 1H), 7.63-7.69 (m, 3H), 7.52-7.54 (d, *J* = 10.5 Hz, 4H), 7.42-7.45 (dd, *J* = 2.0, 10.5 Hz 1H), 7.26-7.31 (m, 1H), 6.84-6.86 (d, *J* = 11 Hz, 2H), 4.13-4.15 (t, *J* = 6 Hz, 2H), 3.58-3.61 (t, *J* = 6 Hz, 2H). ^{13}C NMR (100 MHz, $(CD_3)_2SO$) δ(ppm): 160.97, 154.15, 153.19, 153.11, 151.53, 150.72, 147.72, 147.67, 147.59, 147.52, 146.13, 137.35, 136.62, 131.58, 131.33, 131.18, 130.93, 129.28, 128.54, 128.12, 127.18, 126.83, 126.03, 125.83, 121.81, 121.75, 114.52, 55.82. ESI-HRMS: $[M - 2PF_6]^{2+}$ 432.0944, found 432.0960.

Synthesis of Intermediate **1**

$Ru(phen)_2Cl_2 \cdot 2H_2O$ (0.106 g, 0.2 mmol) and $\mathbf{L_2}$ (0.100 g, 0.21 mmol) were dissolved

in 20 mL ethanol and 10 mL H_2O refluxed 24 h under an argon atmosphere to give a clear red solution. After the solvent was removed, an orange-red powder was obtained. The crude product was purified by column chromatography on a neutral alumina with CH_2Cl_2/CH_3OH (30:1, v/v). The final product (orange-red soild) was obtained by adding saturated aqueous NH_4PF_6 solution dropwise to the solution of the pure product. (Yield = 74 %). ^{1}H NMR (500 MHz, $(CD_3)_2SO$) δ 9.17−9.19 (d, *J* = 9.0 Hz, 1H), 8.74-8.79 (m, 4H), 8.38−8.40 (d, *J* = 13.5 Hz, 4H), 8.05-8.10 (m, 4H), 7.96-7.97 (d, *J* = 6 Hz, 1H), 7.85 (m, 1H), 7.79 (m, 10H), 7.57-7.59 (d, *J* = 10 Hz, 2H), 7.49 (m, 1H), 7.37-7.39 (d, *J* = 11 Hz, 1H), 6.99-7.01 (d, *J* = 10.5 Hz, 2H), 4.2 (t, *J* = 5.5 Hz, 2H), 3.66 (t, *J* =5.5 Hz, 2H). ESI-HRMS: $[M - 2PF_6]^{2+}$ 459.6029, found 459.6027; $[M - PF_6]^+$ 1064.1723, found 1064.1706.

Synthesis of **Ru-tmxf**

Intermediate **1** (0.15 g, 0.163 mmol) and ligand **2** (0.106 g, 0.269 mmol) were dissolved in 12 mL $CHCl_3$, 1 mL ethanol and 1 mL H_2O, then, $CuSO_4 \cdot 5H_2O$ (24.45 mg, 0.098 mmol) and sodium ascorbate (64.58 mg, 0.326 mmol) were added in the pot stirred for 24 hours. The reaction mixture was purified by column chromatography on a neutral alumina with CH_2Cl_2/CH_3OH (40:1, v/v) as eluent. The mainly red band was collected. The final product (orange-red solid) was obtained by adding saturated aqueous NH_4PF_6 solution dropwise to the solution of the pure product. (Yield = 62 %). ^{1}H NMR (500 MHz, $(CD_3)_2SO$) δ(ppm): 9.15−9.17 (d, *J* = 8.0 Hz, 1H), 8.74-8.80 (m, 4H), 8.37−8.40 (d, *J* = 13.5 Hz, 4H), 8.07-8.10 (m, 4H),

8.02-8.05 (m, 2H), 7.95-7.96 (d, *J* = 5 Hz, 1H), 7.82-7.85 (m, 1H), 7.68-7.79 (m, 9H), 7.48-7.53 (m, 3H), 7.33-7.38 (m, 3H), 7.23-7.26 (t, *J* = 7.5 Hz, 1H), 7.16-7.19 (t, *J* = 6.5 Hz, 4H), 7.10-7.11 (d, *J* = 7.5 Hz, 3H), 6.91-6.93 (d, *J* = 9.0 Hz, 2H), 6.71-6.73 (d, *J* = 9.0 Hz, 2H), 6.58-6.59 (d, *J* = 8.5 Hz, 2H), 4.71-4.73 (t, *J* = 5 Hz, 2H), 4.40-4.42 (t, *J* = 5 Hz, 2H), 3.91 (s, 2H), 3.63 (s, 2H), 2.62 (s, 2H), 2.31-2.35 (q, *J* = 7.5 Hz, 2H), 2.17 (s, 3H), 0.78-0.81 (t, *J* = 7 Hz, 3H). ^{13}C NMR (100 MHz, $(CD_3)_2SO$) δ(ppm): 159.58, 153.97, 153.18, 147.72, 147.67, 147.58, 147.51, 146.15, 146.11, 143.73, 142.24, 141.16, 138.37, 137.35, 137.21, 136.61, 131.78, 131.33, 131.19, 130.95, 129.82, 129.39, 129.22, 128.73, 128.55, 128.40, 128.12, 127.12, 126.84, 126.64, 115.05, 113.91, 66.80, 55.07, 49.27, 42.52, 28.95, 13.17. ESI-HRMS: $[M + H - 2PF_6]^{3+}$ 438.4801, found 438.4810; $[M - 2PF_6]^{2+}$ 657.2154, found 657.2182.

Fluorescence Quantum Yield

We use the absolute fluorescence quantum yield apparatus to measure fluorescence quantum yield of **Ru-tmxf** and **Ru-OMe** (0.025 and 0.026) in methanol at the concentration of 5 μM, respectively, and the excitation wavelength is 460 nm.

Two-Photon Absorption Cross Section Measurements

The two-photon luminescence of **Ru-OMe** and **Ru-tmxf** were measured according to the literature methods, Rhodamine B was the reference.[4] The calculation formula was given below:

$$\sigma_S = \sigma_R \frac{\phi_R C_R I_S n_S}{\phi_S C_S I_R n_R}$$

Where σ stands for the TPA cross section, ϕ stands for the quantum yield, *C* stands for the concentration, *n* stands for the refractive index, and *I* stands for the integrated luminescent spectrum. The superscript *S* and *R* represent sample and reference (Rhodamine B).

Singlet Oxygen Generation and Quantum Yield (FD)

The $^1O_2$ quantum yield (FD) was detected according to the literature method,[5] using 1,3-diphenlisobenzofuran (DPBF) as the singlet oxygen capture agent (λ_{ex} = 415 nm, λ_{em} = 480 nm) and $[Ru(bpy)_3]^{2+}$ as the standard (FD = 0.56 in CH_3CN).[6] The emission maxima of DPBF with different irradiation times were obtained, and the singlet oxygen quantum yields were determined using the following equations:

$$-\frac{\Delta[DPBF]}{t} = \frac{I_0 - I_t}{t} = I_{in}\Phi_{ab}\Phi_{\Delta}\Phi_r$$

$$\frac{k}{k^s} = \frac{\Phi_{ab}\Phi_{\Delta}}{\Phi_{ab}^{s}\Phi_{\Delta}^{s}}$$

where I_{in} stands for the incident monochromatic light intensity, Φ_{ab} stands for the light absorbing efficiency, Φ_r stands for the reaction quantum yield of DPBF, t stands for the reaction time, I_0 and I_t stand for the fluorescence intensity before, after irradiation of the complexes, and *k* is the slope of plots. The superscript s stands for the reference.

Cell Culture Conditions

Human breast cancer MCF-7 cells and African green monkey kidney COS-7 cells were maintained in DMEM medium, Human breast cancer MDA-MB-231 cells and Human hepatocyte HL-7702 cells were maintained in RPMI 1640 medium, all of them were supplemented with 1% penicillin-streptomycin and 15% FBS, and atmosphere of 5% CO_2 and 95% air at 37 ℃. When used for imaging, all types of cells were cultured on 35 mm glass-bottom culture dishes for 24 h.

Cellular Uptake

MCF-7 cells were incubated with 3 μM **Ru-tmxf** at 37 ℃ for 0.5, 1, 2.5 h, respectively. MBA-MD-231 cells, HL-7702 cells and COS-7 cells were incubated with 3 μM **Ru-tmxf**, respectively, at 37 ℃ for 2.5 h. After cells were washed with PBS for two times, the confocal luminescence imaging was performed and images were collected (excited at 488 nm, monitored at 570−630 nm).

In Vitro Specificity Studies

MCF-7 cells were pretreated with 0, 25, 50 μM 17*β*-estradiol respectively for 24 h. Next, 3 μM **Ru-tmxf** or **Ru-OMe** were added to the 35 mm glass-bottom culture dishes of MCF-7 cells for a 2.5 h incubation. After cells were washed with PBS for two times, the confocal luminescence imaging was performed and images were collected (excited at 488 nm, monitored at 570−630 nm).

In Vitro Photo-Cytotoxicity Assays

MCF-7 cells were seeded onto 96-well plates at 10000 cells per well and incubated at

37 ºC for 18-24 h. Then different concentrations of **Ru-tmxf** and **Ru-OMe** from 0 to 16 μM in DMEM medium were added to the wells, respectively. To further compare the cytotoxicity of **Ru-tmxf** with **Ru-OMe** plus tamoxifen. Different concentration of **Ru-OMe** plus tamoxifen (concentration ratio was 1:1) from 4 to 16 μM in DMEM medium were added to the wells, too. Then, MCF-7 cells were incubated for 2.5 h. Subsequently, MCF-7 cells treated with **Ru-tmxf**, **Ru-OMe** or **Ru-OMe** plus tamoxifen were subjected to 450 nm light at a power of 20 mW/cm^2 for 10 min. Then the MCF-7 cells were further incubated for 20 h at 37 ºC. Next, adding MTT solution (5 mg/mL) in DMEM to each well. After incubating the cells for 4 h, the solution in each well was removed out carefully, and then adding 100 μL DMSO to each well, and the absorbance at 570 nm was measured with a Bio-Rad microplate reader. The cell viability was obtained by the following equation：

$$cell\ viability\ (\%) = \left(OD_{ps} - \frac{OD_{black\ control}}{OD_{control}} - OD_{black\ control} \right) \times 100\%$$

Confocal Imaging of PDT Induced Cell Death

MCF-7 cell death induced by PDT were detected by Annexin V-FITC/propidium iodide (PI) Apoptosis Detection Kit. Cells were divided into four groups: 1) cells were incubated with 5 μM **Ru-OMe** at 37 ºC for 2.5 h; 2) cells were incubated with 5 μM **Ru-OMe** at 37 ºC for 2.5 h, and then irradiated with 450 nm light (20 mW/cm^2) for 10 min; 3) cells were incubated with 5 μM **Ru-tmxf** at 37 ºC for 2.5 h; 4) cells were incubated with 5 μM **Ru-tmxf** at 37 ºC for 2.5 h, and then irradiated with 450 nm

light (20 mW/cm^2) for 10 min. Whereafter, the cells were further incubated at 37 ºC for 2 h. Then cells were stained with Annexin V-FITC/propidium iodide (PI) Apoptosis Detection Kit according to the manual. The confocal luminescence imaging was performed and images were collected (excited at 488 nm, monitored at 505−545 nm for green channel, 620−680 nm for red channel).

Confocal Imaging of the Selectivity of Phototoxicity

Confocal imaging of PDT induced cell death of MCF-7 cells, MDA-MB-231 cells, HL-7702 cells and COS-7 cells were detected by calcein AM/propidium iodide (PI) Detection Kit. All types of cells were incubated with 5 μM **Ru-tmxf** for 2.5 h, respectively, after being irradiated with 450 nm light (20 mW/cm^2) for 10 min, the cells were further incubated at 37 ºC for 10 h. All the cells were stained with calcein AM/propidium iodide (PI) Detection Kit according to the manual. The living/dead cell imaging was visualized with the excitation wavelength of 488 nm, and the emission wavelength was collected from 515 to 545 nm (green channel) and from 620 to 680 nm (red channel).

Intracellular Singlet Oxygen Detection

DCFH-DA (2,7-dichlorofluorescein diacetate) Detection Kit was used to validate the generation of singlet oxygen in living MCF-7 cells. MCF-7 cells were divided into four groups: 1) untreated groups; 2) cells were incubated with 3 μM **Ru-tmxf** for 2.5 h; 3) cells were incubated with 3 μM **Ru-tmxf** and 150 μM NaN_3 for 2.5 h; 4) cells were incubated with 150 μM NaN_3 for 2.5 h. Then, the cells were washed with PBS

for two times and stained with 10 μM DCFH-DA in serum-free DMEM medium for 20 min at 37 ºC. Subsequently the cells were washed with PBS again, and irradiated with 450 nm light (20 mW/cm^2) for 8 min. Then, confocal luminescence imaging was performed (excited at 488 nm, monitored at 490−520 nm).

Subcellular Localization

MCF-7 cells were cultured on three 35 mm glass-bottom culture dishes for 24 h, then cells were incubated with 3 μM **Ru-tmxf** for 2.5 h, after cells were washed with PBS for three times, LysoTracker Green DND 26 (100 nM), Hoechst 33342 (2 μg/mL) and MitoTracker Green FM (100 nM) was added respectively and the cells were incubated for 20 min. Next, the confocal luminescence imaging was performed.

Lysosomes Disruption Assay

MCF-7 cells were incubated with different following treatments: 1) untreated; 2) irradiated with 450 nm light (20 mW/cm^2) for 10 min; 3) incubated with 3 μM **Ru-tmxf** for 2.5 h; 4) incubated with 3 μM **Ru-tmxf** for 2.5 h and then irradiated with 450 nm light (20 mW/cm^2); 5) incubated with 3μM **Ru-OMe** for 2.5 h; 6) incubated with 3 μM **Ru-OMe** for 2.5 h and then irradiated with 450 nm light (20 mW/cm^2). After treatment, cells were incubated with acridine orange (5 μM) for 20 min and subjected to confocal luminescence imaging. The confocal luminescence imaging was performed and images were collected (excited at 488 nm, monitored at 505−545 nm for green channel, 617-640 nm for red channel).

Analysis of mitochondrial transformation during PDT process

MCF-7 cells were incubated with different following treatments: 1) untreated; 2) incubated with 3 μM **Ru-tmxf** for 2.5 h; 3) irradiated with 450 nm light (20 mW/cm^2) for 10 min; 4) incubated with 3 μM **Ru-tmxf** for 2.5 h and then irradiated with 450 nm light (20 mW/cm^2). After treatment, all the cells were stained with JC-1 Detection Kit according to the manual. The confocal luminescence imaging was performed and images were collected (excited at 488 nm and 559 nm, monitored at 515−545 nm for green channel, 590-640 nm for red channel).

Cells in Group 4 were incubated with MitoTracker Green FM (100 nM) and the confocal luminescence imaging was performed. (excited at 488 nm and 559 nm, monitored at 515−545 nm for green channel, 590-640 nm for red channel).

JC-1 is a dual-emission potential-sensitive probe, at higher potentials of mitochondria in living cells, JC-1 forms red-fluorescent "J-aggregates" (J-A), while red-fluorescent disappearing and a green-fluorescent monomer (J-M) can be formed in low mitochondrial membrane potential cells.[7] Thus we firstly used JC-1 Detection Kit to investigate whether mitochondrial membrane potential (MMP) was changed or not during the PDT process of **Ru-tmxf**. As shown in Fig. S9, compared with the untreated group, bright red fluorescence and negligible green fluorescence from the mitochondria in the groups treated with **Ru-tmxf**, light and PDT, respectively, was also observed obviously, demonstrating that JC-1 could highly aggregate (red channel) in these groups.

Then, we used mitochondria specific tracker MitoTracker Green and JC-1 to label mitochondria of MCF-7 cells after PDT process. As shown in Fig. S10, MitoTracker Green and JC-1 overlapped well in MCF-7 cells after PDT, which demonstrated that the mitochondria of MCF-7 cells were not disrupted remarkably after PDT treatment.

Two-Photon Excited Confocal Imaging

MCF-7 cells were further incubated with **Ru-tmxf** (3 μM) for 2.5 h. The cell imaging was visualized under one-photon and two-photon excitation. The excitation wavelength was 488 nm or 830 nm (fs), and the emission wavelength was collected from 570 to 630 nm (red channel).

$^1O_2$ Generation under Two-Photon Irradiation

$^1O_2$ generation under two-photon irradiation was also detected by DCFH-DA (2, 7-dichlorofluorescein diacetate) Detection Kit. MCF-7 cells were divided into two groups: 1) untreated groups; 2) cells were incubated with 3 μM **Ru-tmxf** for 2.5 h. Then, the cells were washed with PBS for three times and stained with 10 μM DCFH-DA in serum-free DMEM medium for 20 min at 37 ºC. Subsequently the cells were washed three times with PBS again, and subjected to two-photon irradiation at 830 nm for 3 min using a confocal multiphoton microscope (Olympus, FV1000) with a high-performance mode-locked titanium-sapphire laser source (MaiTai, Spectra-Physics, U.S.A.). Then, confocal fluorescence imaging was performed to give the level of intracellular singlet oxygen with the excitation wavelength of 488 nm and emission wavelength from 480 nm to 520 nm.

Photo-Cytotoxicity under Two-Photon Irradiation

Confocal imaging of two-photon PDT induced cell death of MCF-7 cells were detected by calcein AM/propidium iodide (PI) Detection Kit. Cells were divided into two groups: 1) untreated; 2) cells were incubated with 3 μM **Ru-tmxf** for 2.5 h. Both of the two groups were irradiated with two-photon laser for 5 min using a confocal multiphoton microscope (Olympus, FV1000) with a high-performance mode-locked titanium-sapphire laser source (MaiTai, Spectra-Physics, U.S.A.). Subsequently, the cells were further incubated at 37 ºC for 10 h. All the cells were stained with calcein AM/propidium iodide (PI) Detection Kit according to the manual. The living/dead cell imaging was visualized with the excitation wavelength of 488 nm, and the emission wavelength was collected from 515 to 545 nm (green channel) and from 620 to 680 nm (red channel).

Content

Fig. S14 ESI-MS of $\mathbf{L_2}$.

Fig. S15 ^{1}H NMR spectrum of $\mathbf{L_2}$.

Fig. S16 ESI-HRMS of **1**.

Fig. S17 ^{1}H NMR spectrum of **1**.

Fig. S18 ESI-HRMS of **2**.

Fig. S19 ^{1}H NMR spectrum of **2**.

Fig. S20 ESI-HRMS of **Ru-OMe**.

Fig. S21 ^{1}H NMR spectrum of **Ru-OMe**.

Fig. S22 ^{13}C NMR spectrum of **Ru-OMe**.

Fig. S23 ESI-HRMS of **Ru-tmxf**.

Fig. S24 ^{1}H NMR spectrum of **Ru-tmxf**.

Fig. S25 ^{13}C NMR spectrum of **Ru-tmxf**.

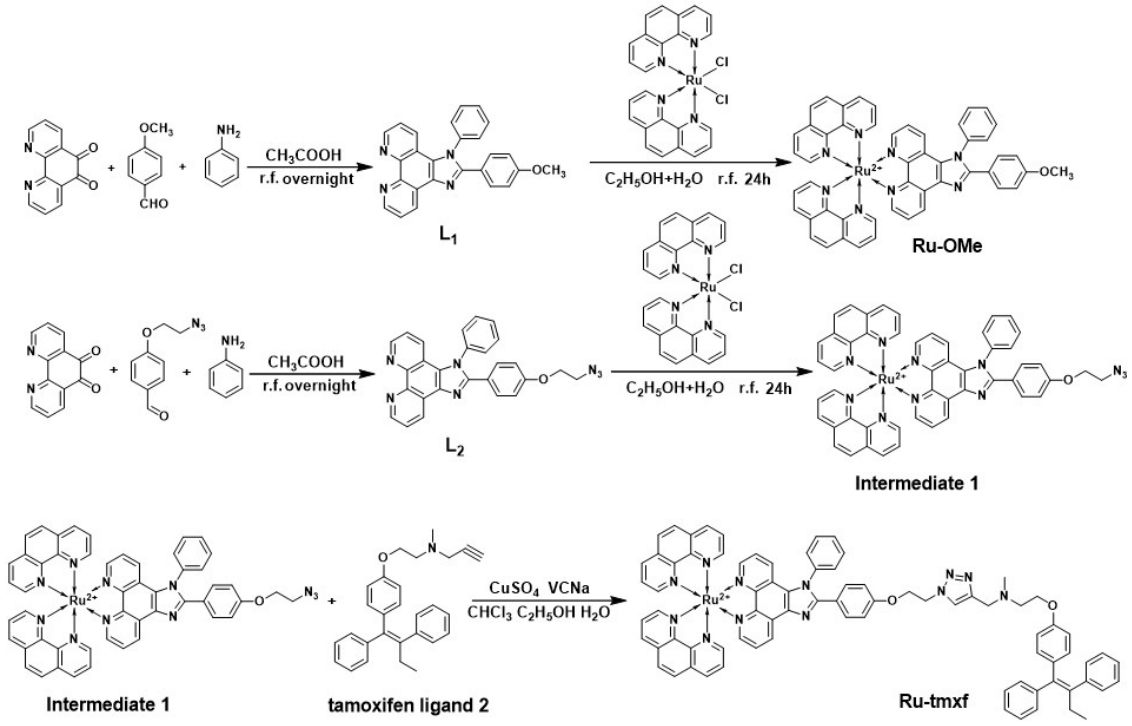

Scheme S1 Synthesis routes of **Ru-OMe** and **Ru-tmxf**.

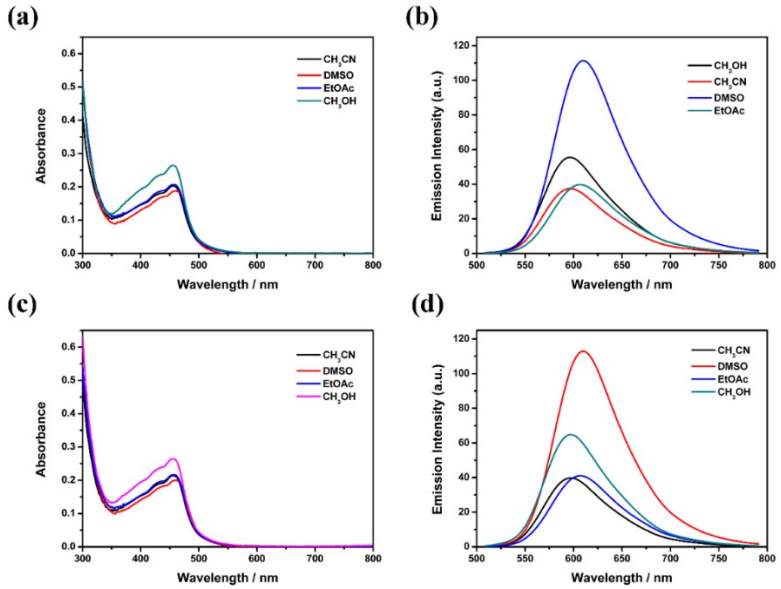

Fig. S1 (a), (b) Absorption and Emission spectra of **Ru-OMe** in different solvents; (c), (d) Absorption and Emission spectra of **Ru-tmxf** in different solvents.

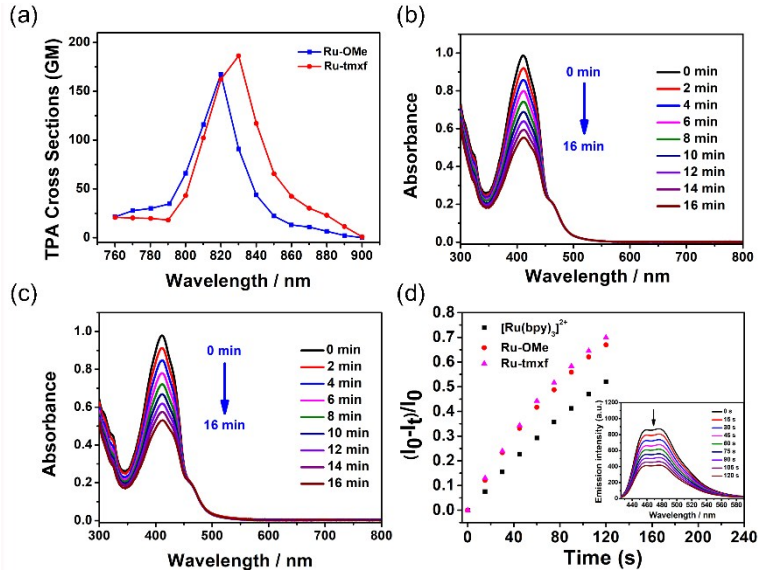

Fig. S2 (a) Two-photon action absorption cross sections of Ru complexes at different excitation wavelengths from 760 to 900 nm; (b) and (c) Absorption spectra of DPBF with **Ru-tmxf** and **Ru-OMe** in CH_3OH; (d) $^1O_2$ quantum yield (Φ_Δ) of **Ru-OMe** and **Ru-tmxf** via changes of the emission by DPBF versus irradiation time in CH_3CN.

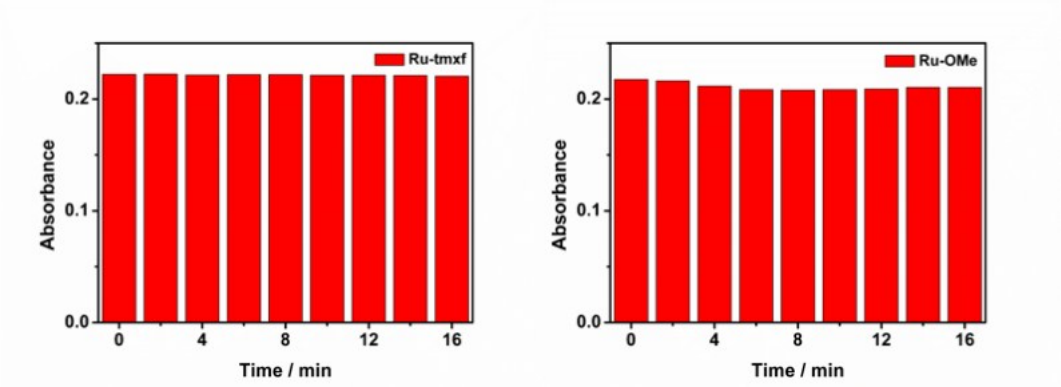

Fig. S3 Absorbance of **Ru-tmxf** and **Ru-OMe** at 458 nm in CH_3OH.

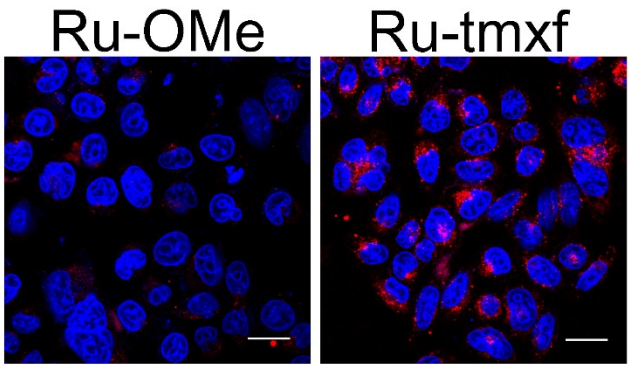

Fig. S4 Confocal luminescence imaging of MCF-7 cells incubated with **Ru-OMe** (3 μM) and **Ru-tmxf** (3 μM) for 2.5h. Scale bars are 30 μm.

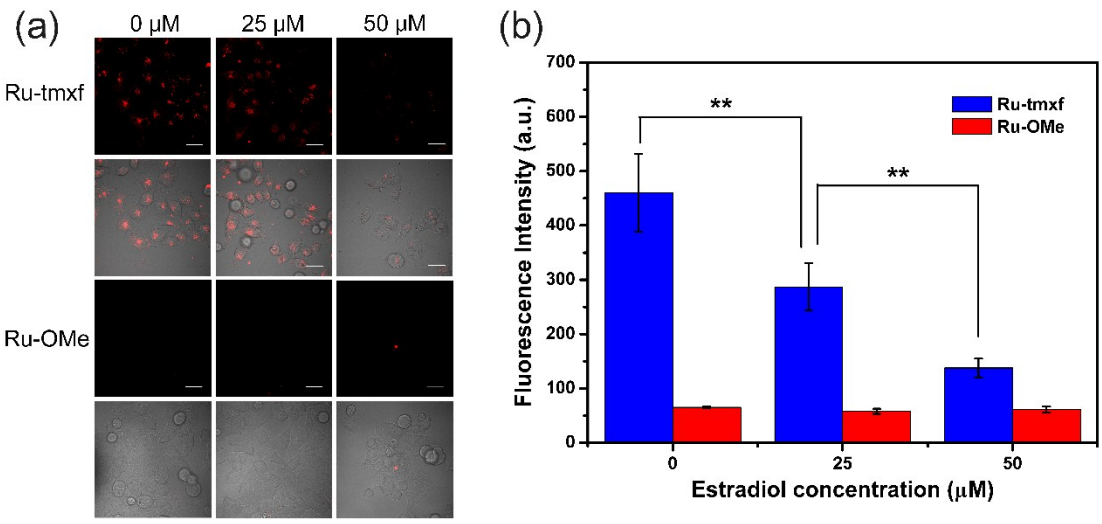

Fig. S5 (a) Confocal luminescence imaging of MCF-7 cells pre-treated with 17*β*-estradiol (0, 25, 50 μM) incubated with **Ru-tmxf** or **Ru-OMe** for 2.5 h. Ex: 488 nm, Em: 570-630 nm. Scale bars are 30 μm. (b) Fluorescence intensity in MCF-7 cells under the same conditions with (a).

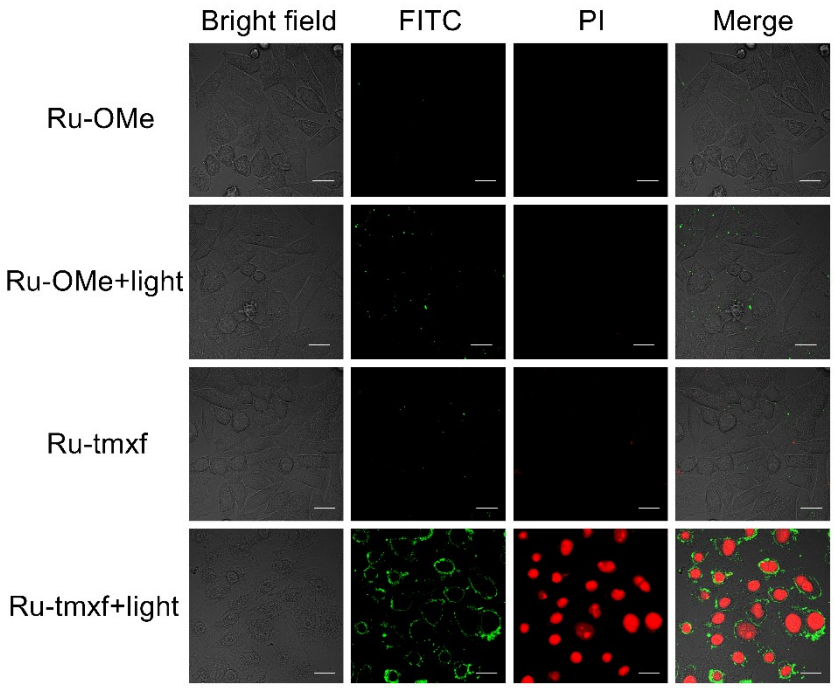

Fig. S6 Confocal luminescence imaging of Annexin -FITC and PI labelled MCF-7

cells with different treatments. λ_{ex}: 488 nm, λ_{em}: 505-545 nm (FITC); 620-700 nm (PI). Scale bars: 20 μm.

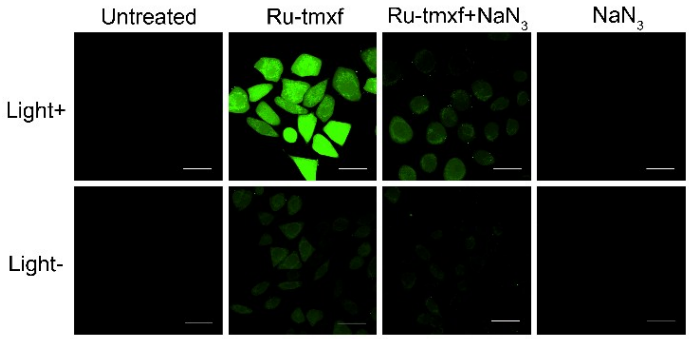

Fig. S7 Confocal luminescence imaging of intracellular $^1O^2$ production by **Ru-tmxf** in MCF-7 cells under light conditions (12 J/cm^2) using DCFH-DA assay. λex: 488 nm, λem: 490-520 nm (DCF). Scale bars: 30 μm.

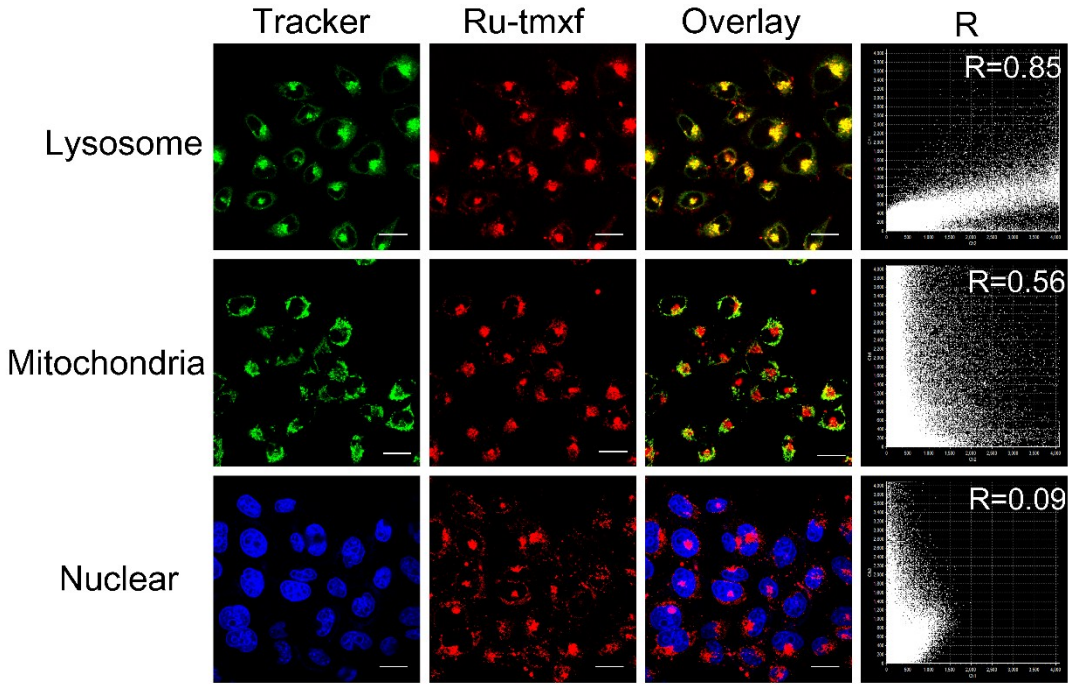

Fig. S8 Subcellular colocalization images of **Ru-tmxf** (3 μM) in MCF-7 cells with LysoTracker Green, MitoTracker Green and Hoechst 33342 staining. Ex: 488 nm, Em:

515-545 nm (LysoTracker Green); Ex: 488 nm, Em: 515-545 nm (MitoTracker Green). Ex: 405 nm, Em: 440-480 nm (Hoechst 33342); Ex: 488 nm, Em: 570-630 nm (MitoTracker Green). Scale bars: 30 μm.

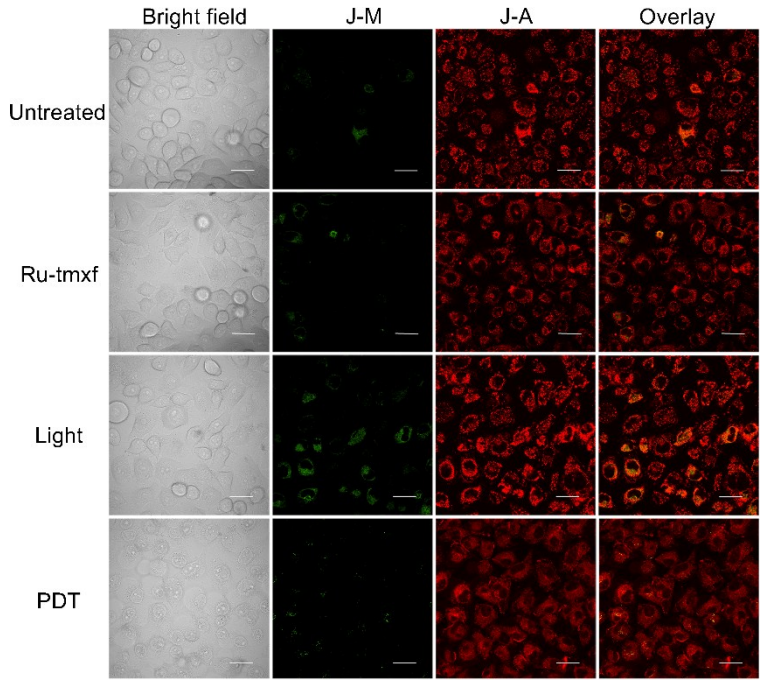

Fig. S9 Confocal luminescence imaging of JC-1 labelled MCF-7 cells with different treatments. λ_{ex}: 488 nm and 559 nm, λ_{em}: 515-545 nm (green channel); 590-630 nm (red channel). Scale bars: 30 μm.

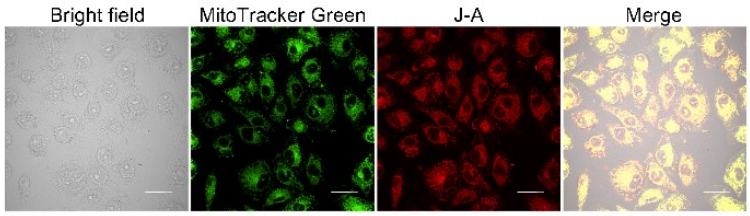

Fig. S10 Confocal luminescence imaging of MitoTracker Green and JC-1 labelled MCF-7 cells after PDT treatments. λ_{ex}: 488 nm and 559 nm, λ_{em}: 515-545 nm (green channel); 590-630 nm (red channel). Scale bars: 30 μm.

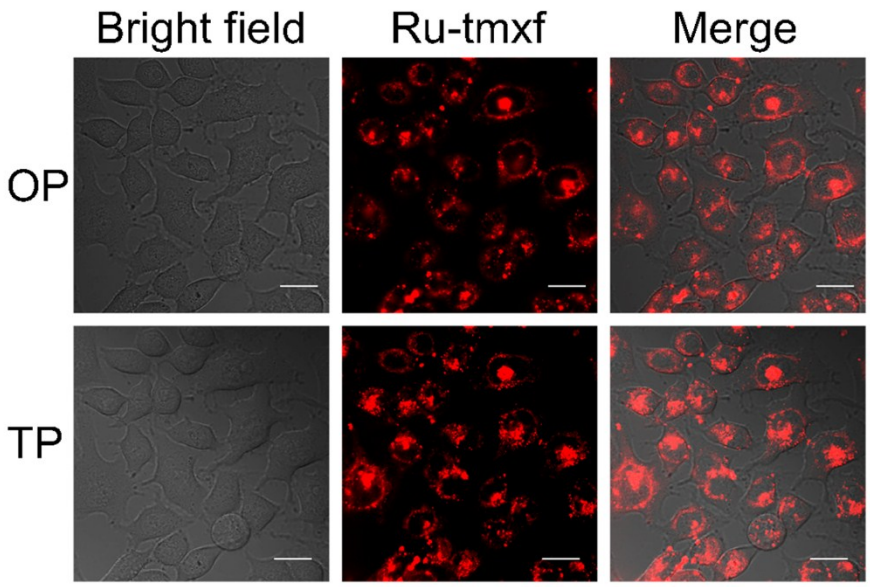

Fig. S11 (a) OP and TP luminescence images of **Ru-tmxf** in MCF-7 cells. λ_{ex}: 488 nm (OP), 830 nm (TP); λ_{em}: 570-630 nm. Scale bars: 30 μm.

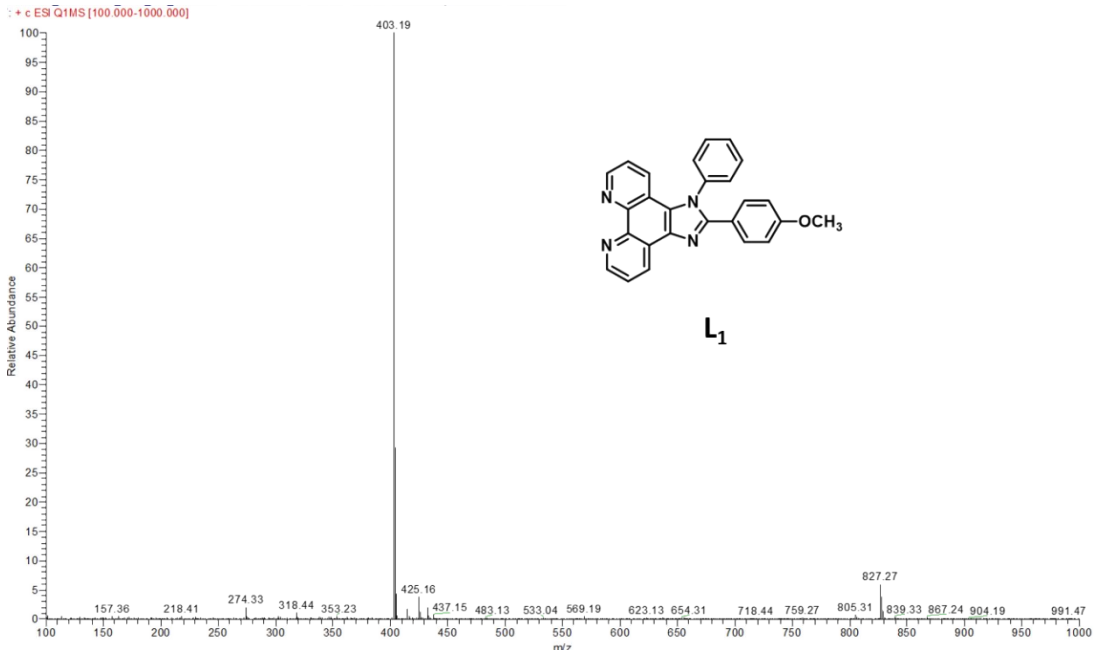

Fig. S12. ESI-MS spectrum of $\mathbf{L_1}$.

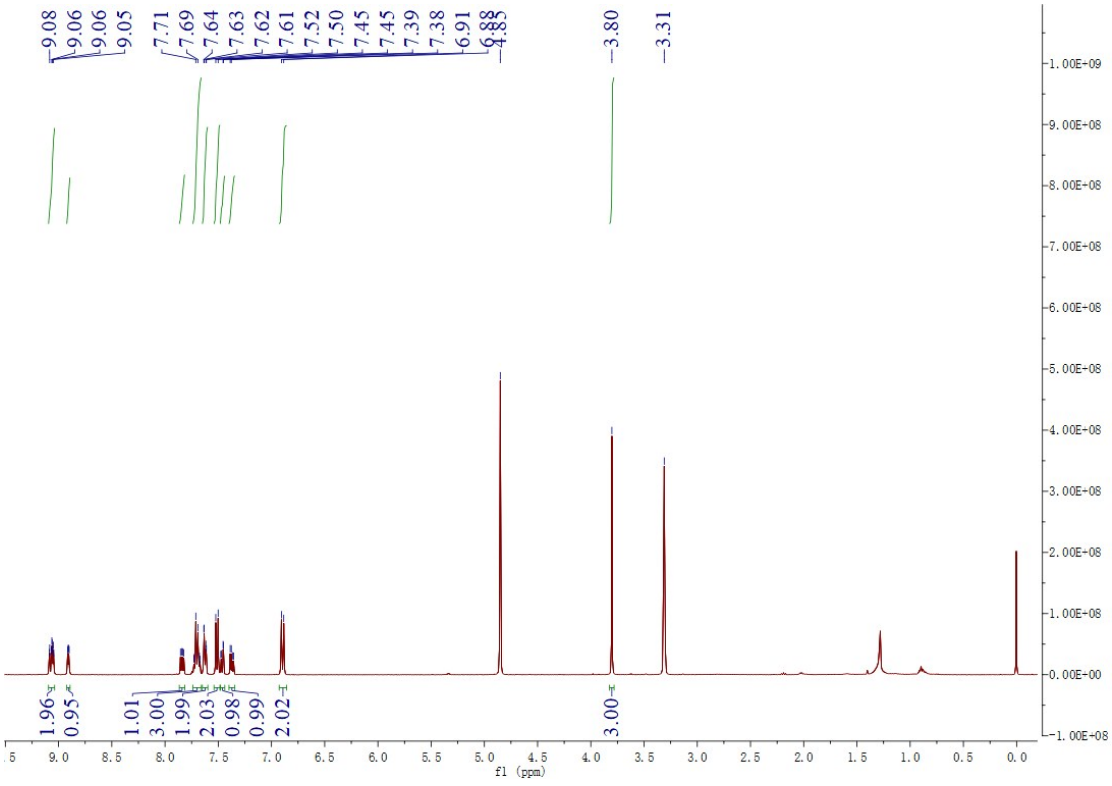

Figure S13. ^{1}H NMR spectrum of $\mathbf{L_1}$.

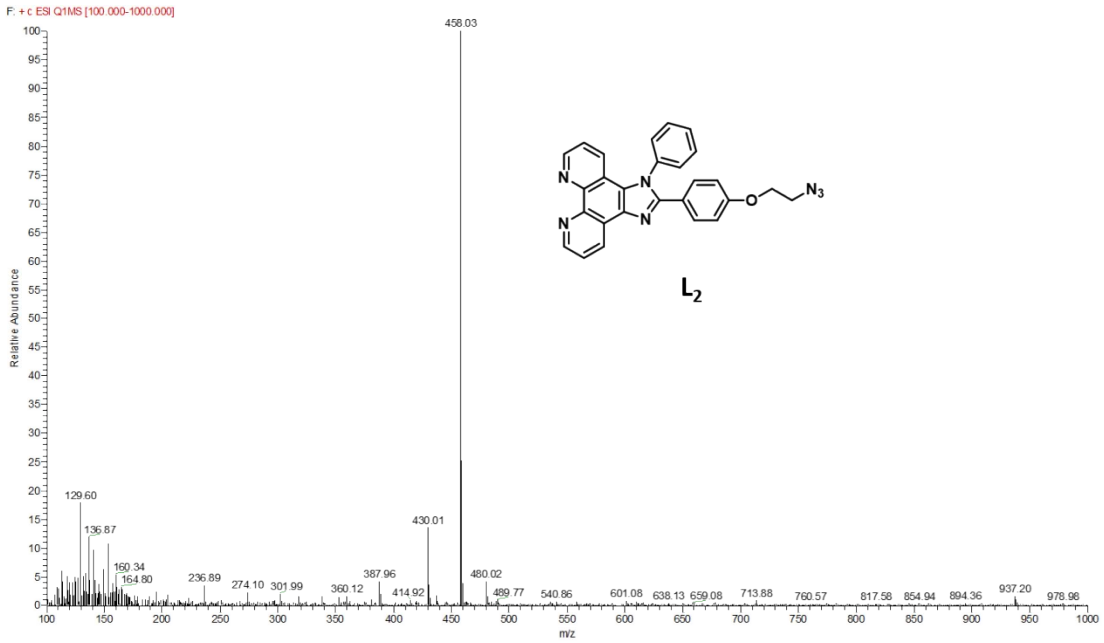

Figure S14. ESI-MS spectrum of $\mathbf{L_2}$.

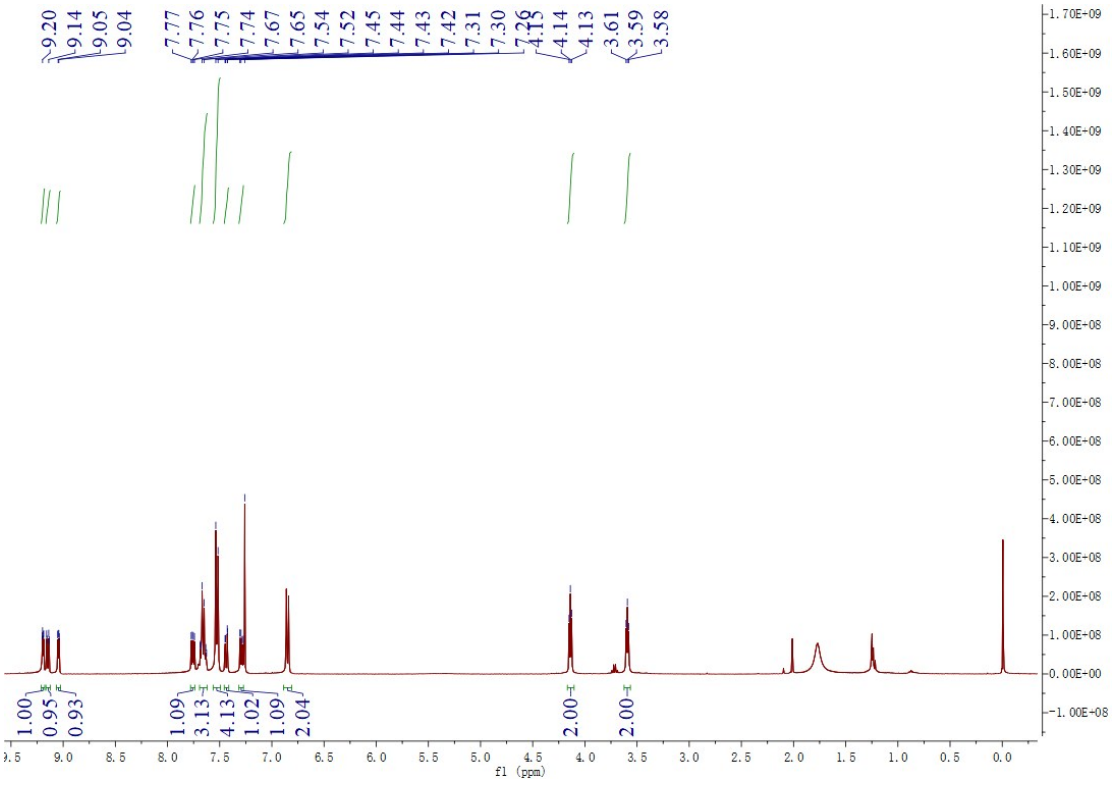

Figure S15. ^{1}H NMR spectrum of $\mathbf{L_1}$.

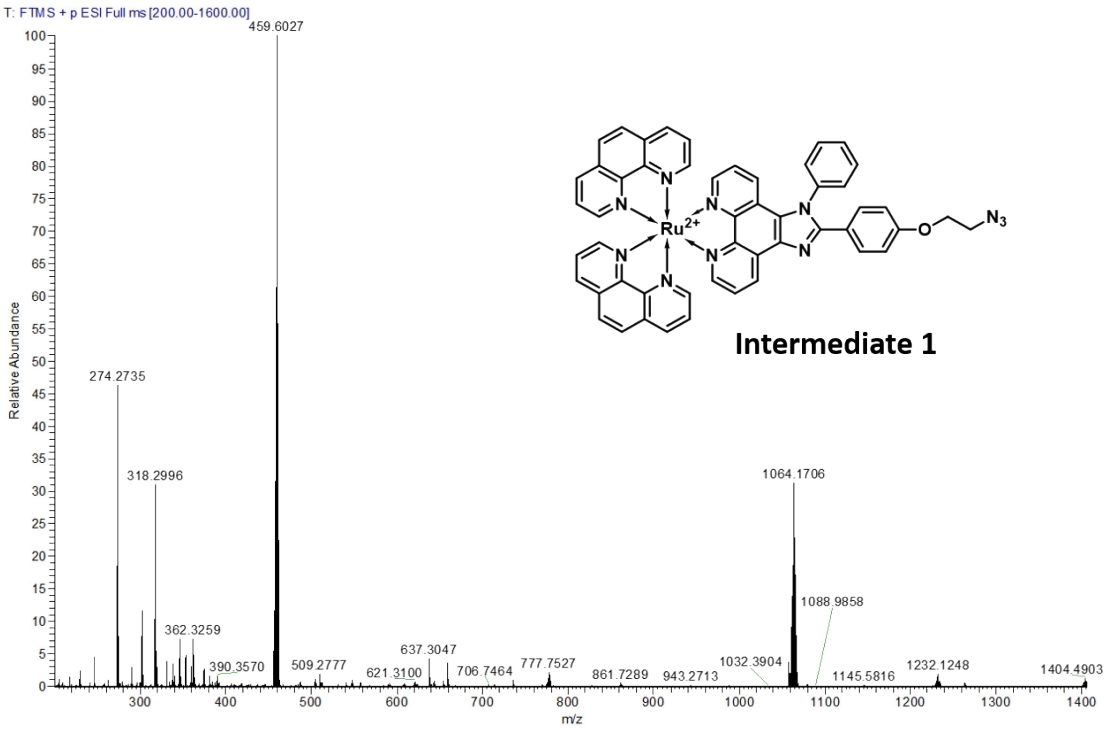

Figure S16. ESI-HRMS spectrum of **1**.

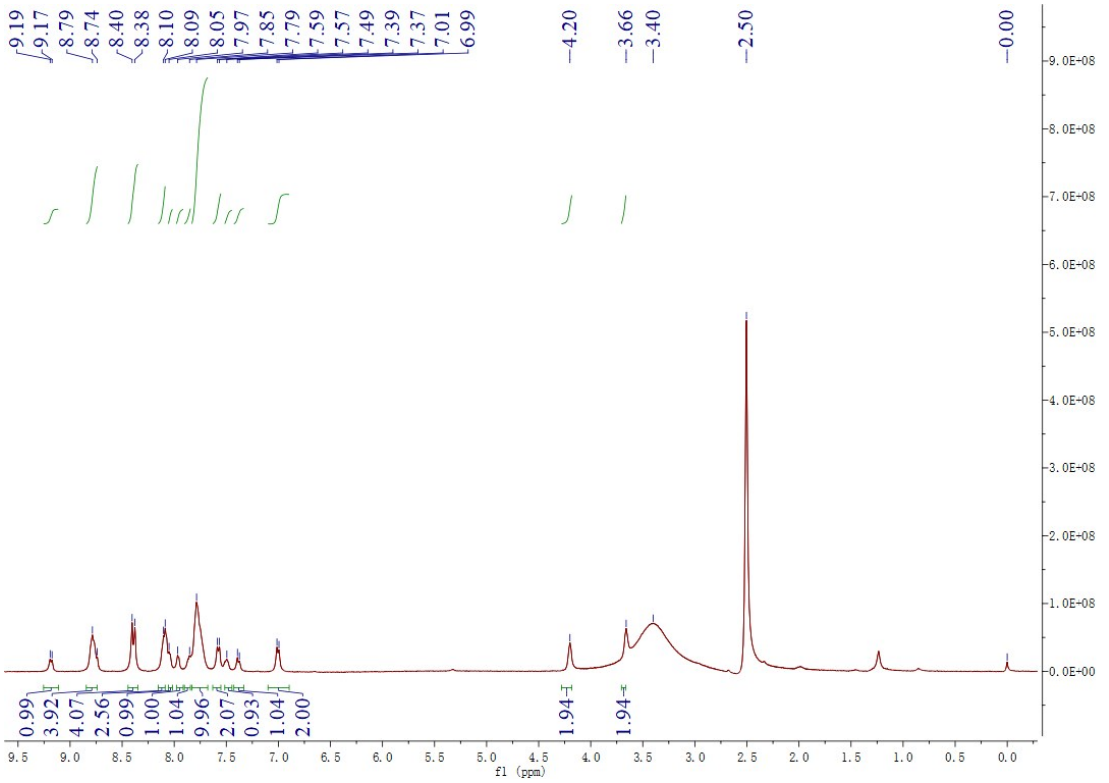

Figure S17. ^{1}H NMR spectrum of **1.**

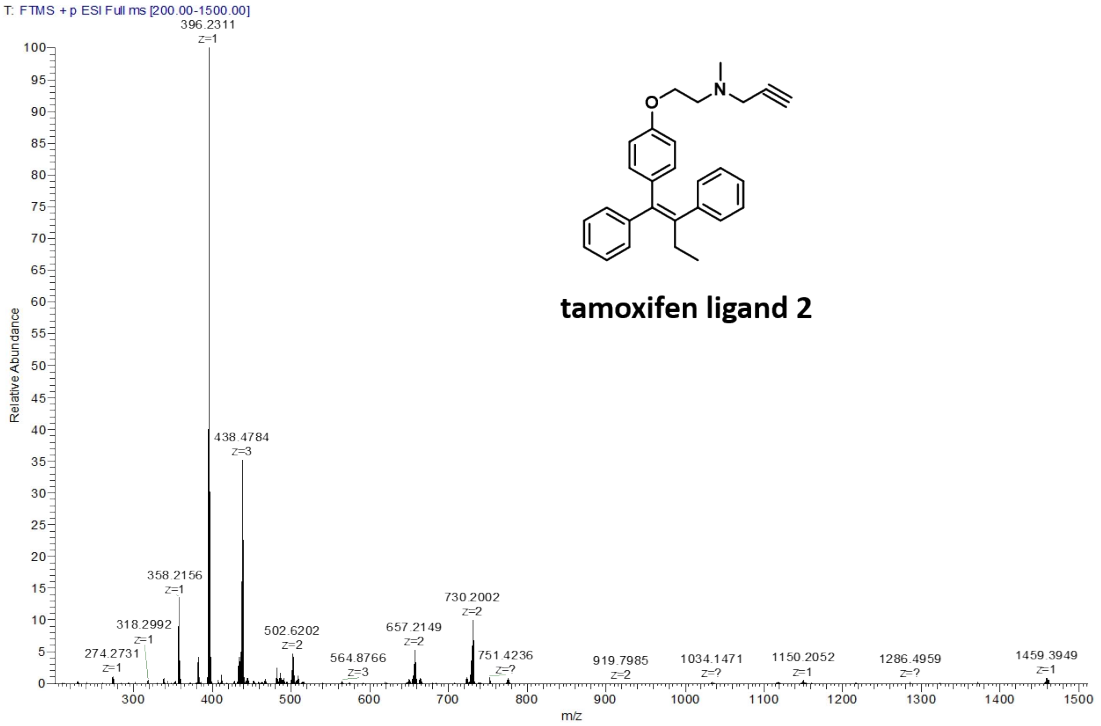

Figure S18. ESI-HRMS spectrum of **2**.

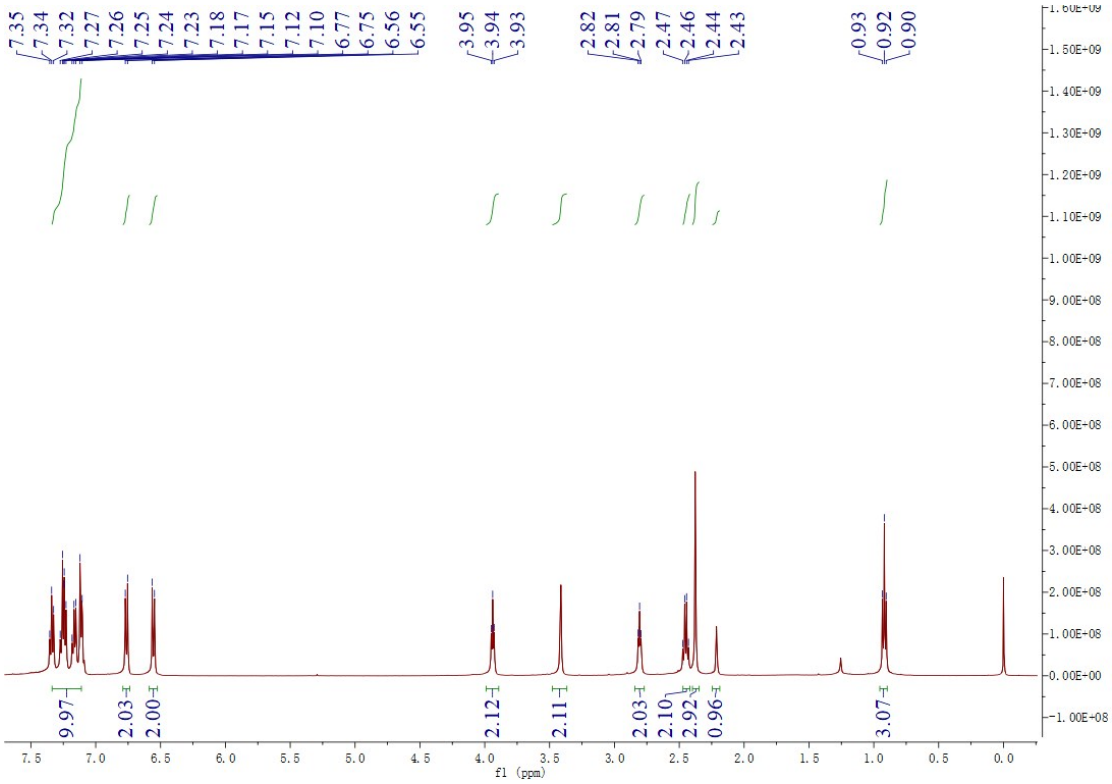

Figure S19. ^{1}H NMR spectrum of **2**.

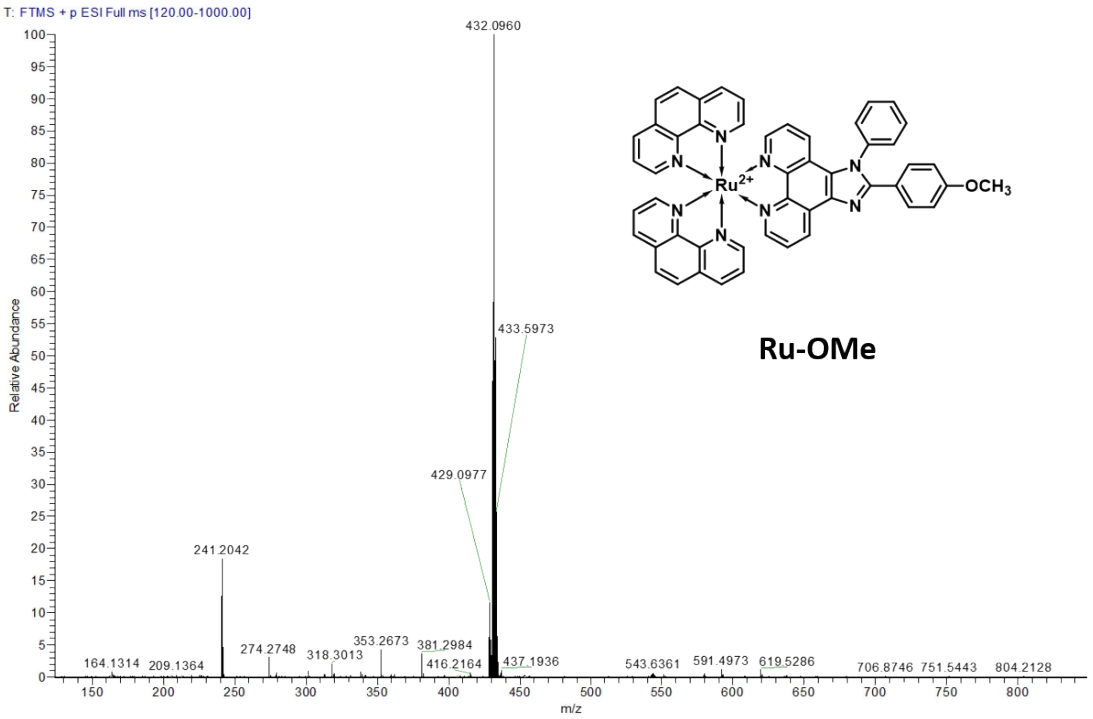

Figure S20. ESI-HRMS spectrum of **Ru-OMe**.

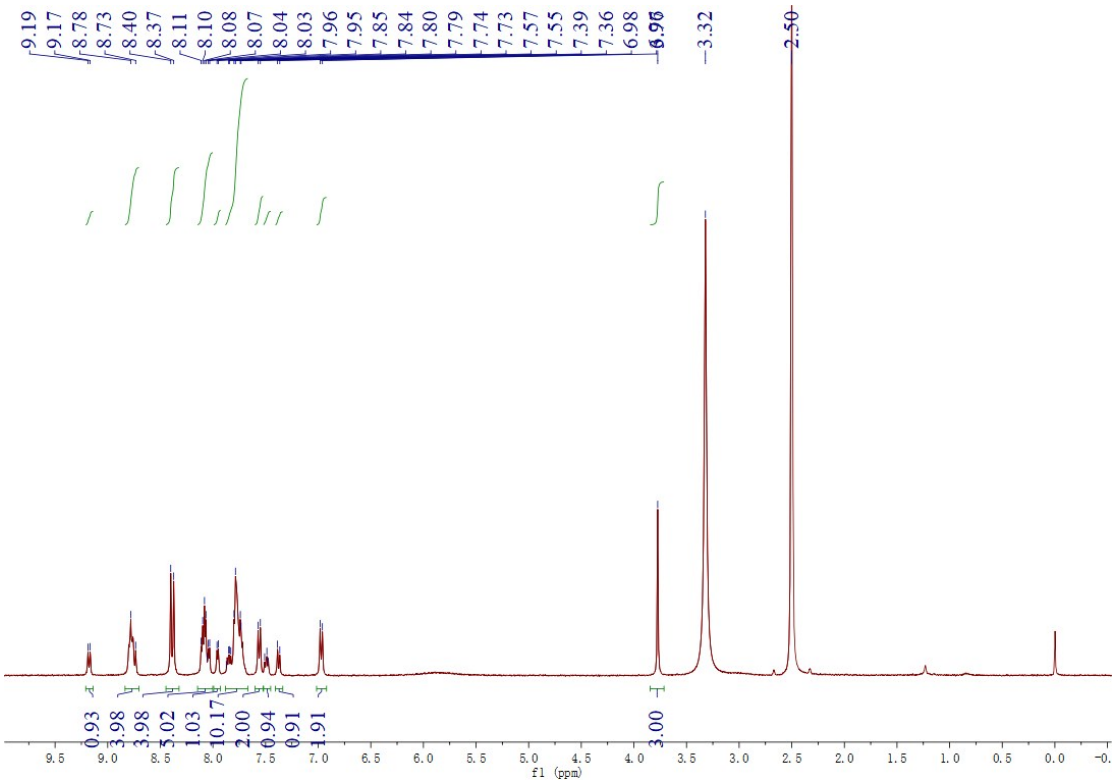

Figure S21. ^{1}H NMR spectrum of **Ru-OMe**.

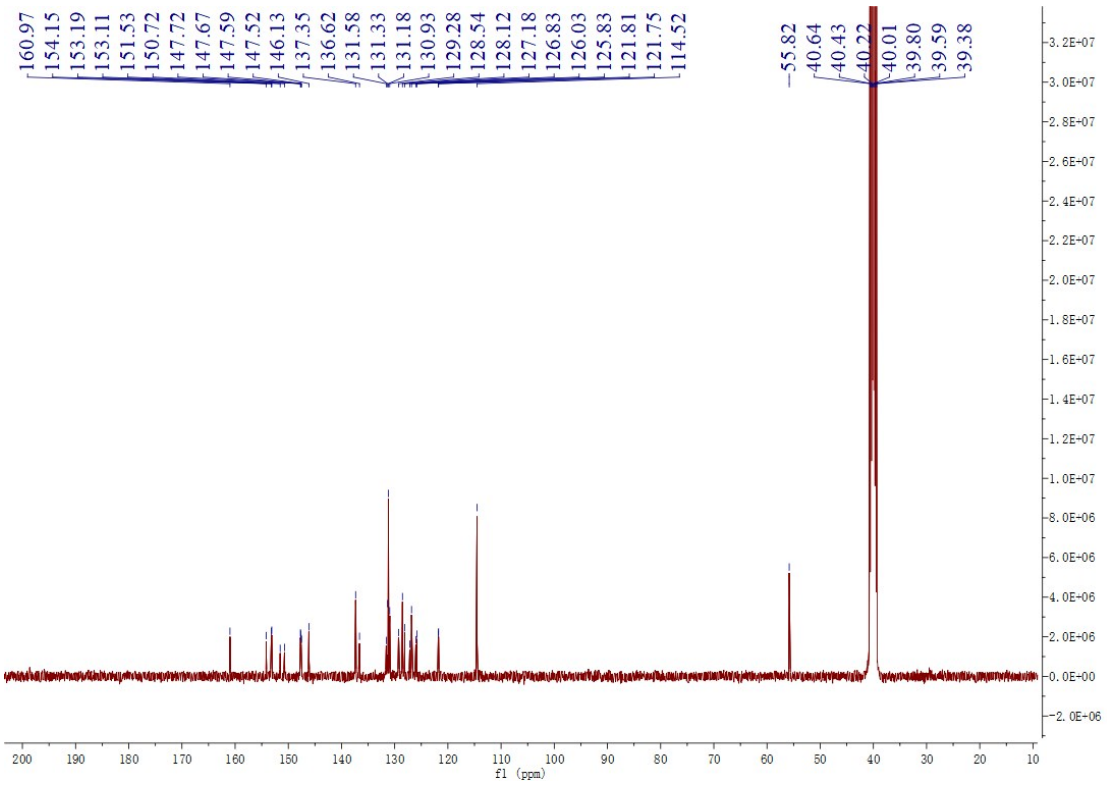

Figure S22. ^{13}C NMR spectrum of **Ru-OMe**.

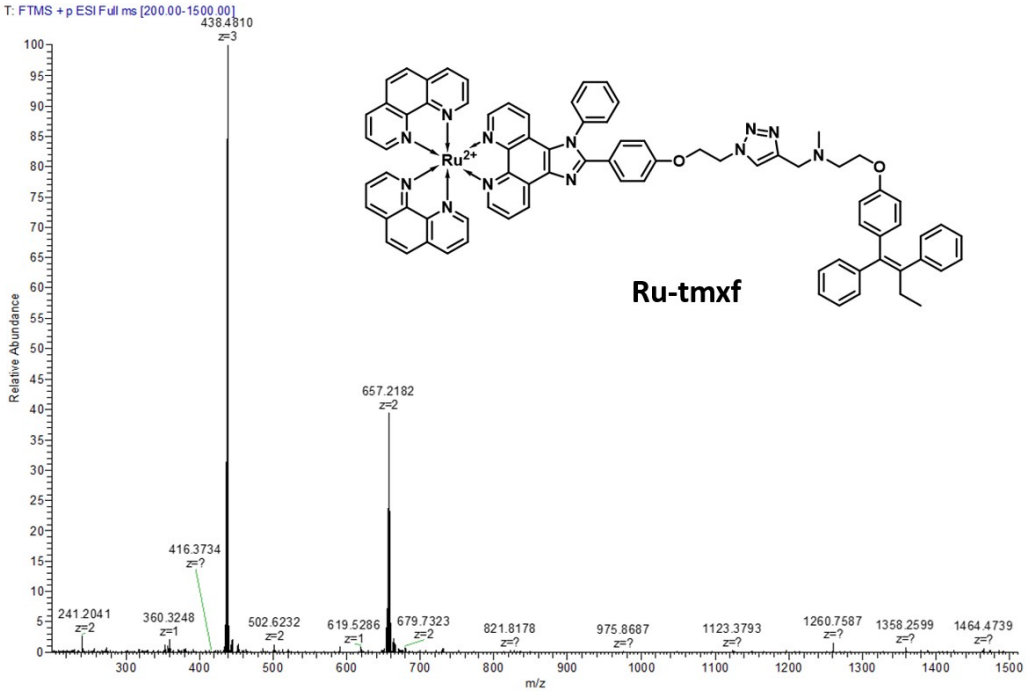

Figure S23. ESI-HRMS spectrum of **Ru-tmxf**.

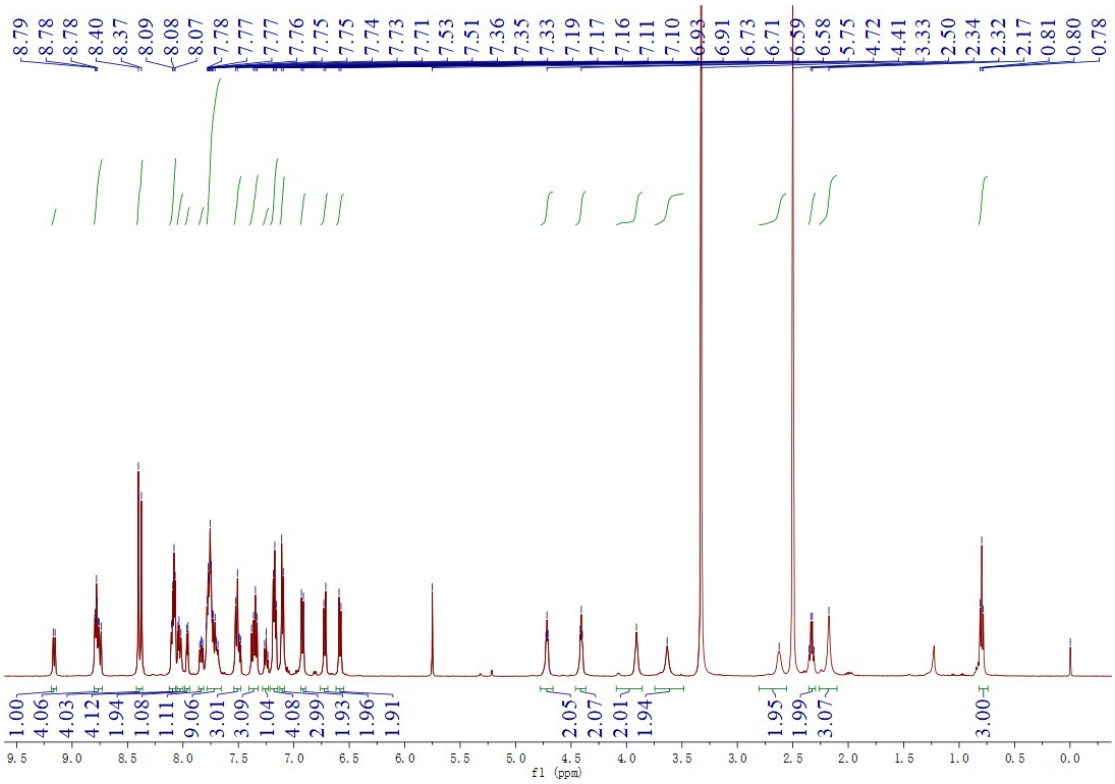

Figure S24. ^{1}H NMR spectrum of **Ru-tmxf**.

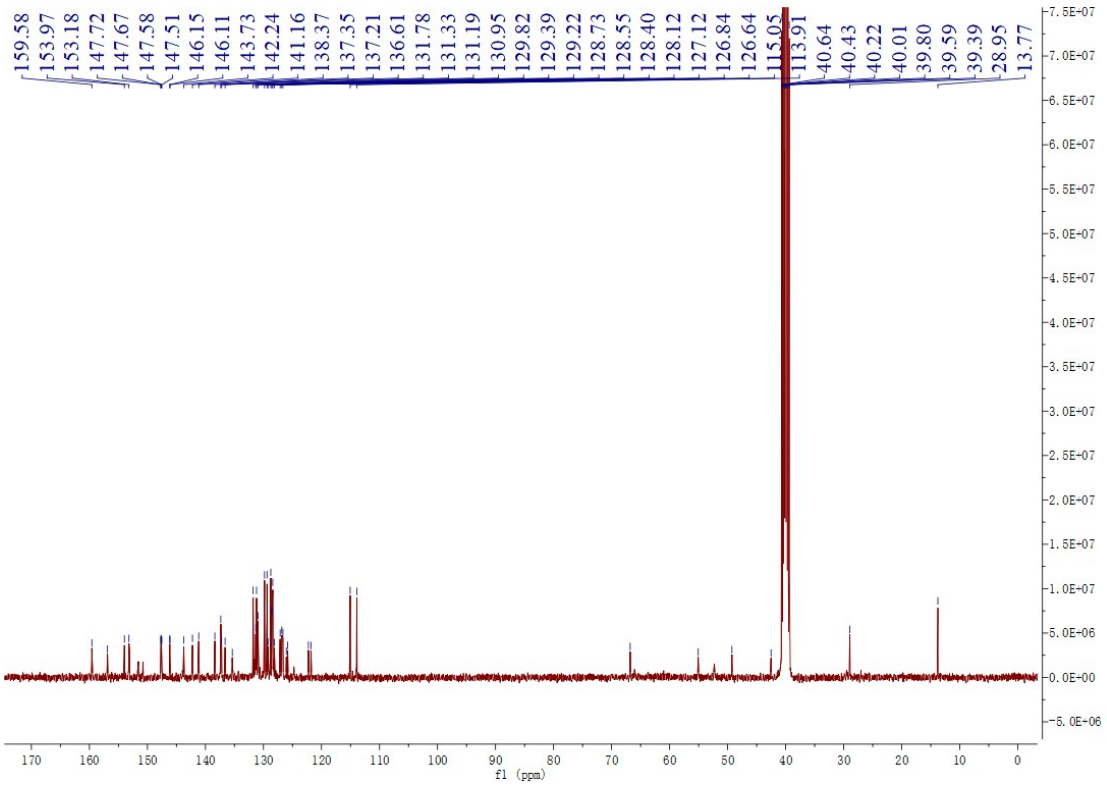

Figure S25. ^{13}C NMR spectrum of **Ru-tmxf**.

References

1 F.-L. Zhang, M.-R. Song, G.-K. Yuan, H.-N. Ye, Y. Tian, M.-D. Huang, J.-P. Xue, Z.-H. Zhang and J.-Y. Liu, *J. Med. Chem.*, 2017, **60**, 6693.

2 B. P. Sullivan, D. J. Salmon and T. J. Meyer, *Inorg. Chem.*, 1978, **17**, 3334.

3 M. D. P. Risseeuw, D. J. H. De Clercq, S. Lievens, U. Hillaert, D. Sinnaeve, F. Van den Broeck, J. C. Martins, J. Tavernier and S. Van Calenbergh, *Chemmedchem*., 2013, **8**, 521.

4 C. Xu, W. W. Webb, *J. Opt. Soc. Am. B.*, 1996, **13**, 481.

5 C. Zhang, J. Zhao, S. Wu, Z. Wang, W. Wu, J. Ma, S. Guo and L. Huang, *J. Am. Chem. Soc.*, 2013, **135**, 10566.

6 J. Hess, H. Huang, A. Kaiser, V. Pierroz, O. Blacque, H. Chao and G. Gasser, *Chem. Eur. J.*, 2017, **23**, 9888.

7 Z. Lv, H. Wei, Q. Li, X. Su, S. Liu, K. Y. Zhang, W. Lv, Q. Zhao, X. Li, W. Huang, *Chem. Sci.*, 2018, **9**, 502.